

Externally Valid Policy Evaluation Combining Trial and Observational Data

Sofia Ek

Uppsala University, Sweden

Dave Zachariah

Uppsala University, Sweden

Abstract

Randomized trials are widely considered as the gold standard for evaluating the effects of decision policies. Trial data is, however, drawn from a population which may differ from the intended target population and this raises a problem of external validity (aka. generalizability). In this paper we seek to use trial data to draw valid inferences about the outcome of a policy on the target population. Additional covariate data from the target population is used to model the sampling of individuals in the trial study. We develop a method that yields certifiably valid trial-based policy evaluations under any specified range of model miscalibrations. The method is nonparametric and the validity is assured even with finite samples. The certified policy evaluations are illustrated using both simulated and real data.

1 Introduction

Randomized controlled trials (RCT) are often considered to be the ‘gold standard’ when evaluating the effects of different decisions or, more generally, decision policies. RCT studies circumvent the need to identify and model potential confounding variables that arise in observational studies. Trial studies enable the evaluation and learning of decision policies for use in, e.g., clinical decision support, precision medicine and recommendation systems (Qian & Murphy, 2011; Zhao et al., 2012; Kosorok & Laber, 2019).

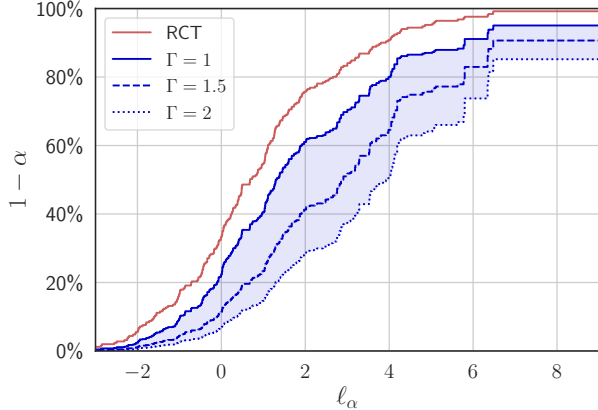
However, RCTs sample individuals that may differ systematically from a target population of interest. For instance, clinical trials usually involve only individuals who do not have any relevant comorbidities and those who volunteer for trials may very well exhibit different characteristics than the target population. It is also common that studies are limited to a specific geographical area, even when the intended target is

a broader region. Invalid inferences about a decision policy can be potentially harmful in safety-critical applications, where the cautionary principle of “above all, do no harm” applies (Smith, 2005). This is especially challenging since the distributions of population characteristics are unknown. How can we *generalize* results from the trial sample to the intended population?

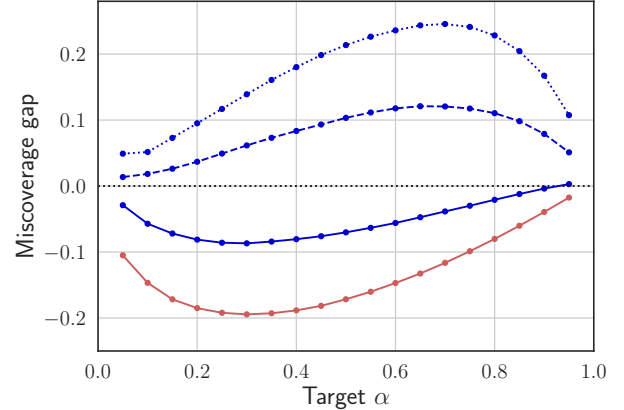
The focus of this paper is the problem of establishing *externally* valid inferences about outcomes in a target population, when using experimental results from a trial population (Campbell & Stanley, 1963; Manski, 2007; Westreich, 2019). We consider evaluating a decision policy, denoted π , that maps covariates X of an individual onto a recommended action A . The outcome of this decision has an associated loss L (aka. disutility or negative reward). We assume the availability of samples (X, A, L) from the trial population as well as covariate data X from the target population (Lesko et al., 2016; Li et al., 2022; Colnet et al., 2020). The covariate data is used to model the sampling of individuals in the trial study. We propose a method for evaluating policy π that

- is nonparametric and makes no assumptions about the distributional forms of the data,
- takes into account possible covariate shifts from trial to target distribution, even when using miscalibrated sampling models,
- and certifies valid finite-sample inferences of the out-of-sample loss, up to any specified degree of model miscalibration.

Many policy evaluation methods are focused on estimating the expected loss $\mathbb{E}_\pi[L]$ of π . However, since a substantial portion of losses L may exceed the mean, this focus can miss important tail events (Wang et al., 2018; Huang et al., 2021). By contrast, evaluating a policy in terms of its out-of-sample loss provides a more complete characterization of its performance and is consonant with the cautionary principle. Figure 1 illustrates the evaluation of π using limit curves which



(a)



(b)

Figure 1: Inferring the out-of-sample losses of a policy π . (a) The loss L is bounded by an upper limit ℓ_α with a probability of at least $1 - \alpha$. The RCT-based limit curve uses only trial data, whereas the other limit curves also utilize a sampling model trained using additional covariate data X from the target population. Each limit curve in blue is certified to provide valid inferences for models miscalibrated up to a degree Γ defined in (3). (b) Gap between the actual probability of exceeding the limit, $L > \ell_\alpha$, and the nominal probability of miscoverage α . A negative gap means the inference ℓ_α is *invalid*, while a positive gap implies it is *valid* but conservative. Details of the experiment are presented in Section 5.1.

upper bound the out-of-sample loss L with a given probability $1 - \alpha$. A limit curve based on RCT-data alone is only ensured to be valid for a trial population. Using additional covariate data, however, we can certify the validity of the inferences for the target population up to any specified degree of miscalibration of the sampling model.

The rest of the paper is outlined as follows. We first state the problem of interest in Section 2 and relate it to the existing literatures in Section 3. We then propose a policy evaluation method in Section 4 and demonstrate its properties using both synthetic and real data in Section 5. We conclude the paper with a discussion in Section 6 about the properties of the method and some future directions of research.

2 Problem Formulation

Any policy π , whether deterministic or randomized, can be described by a distribution $p_\pi(A|X)$. Each covariate $X \in \mathbb{R}^p$ and action A has an associated loss $L \in \mathbb{R}$. We consider here a discrete action space, i.e. $A \in \{1, \dots, K\}$. The decision process has a causal structure that can be formalized by a directed acyclic graph, visually summarized in Figure 2 (Peters et al., 2017). The sampling indicator S indicates whether individuals are drawn from a *target* population, $S = 0$, or a *trial* population, $S = 1$. This may depend on their characteristics associated with X . The causal structure allows to decompose the two distributions. The target

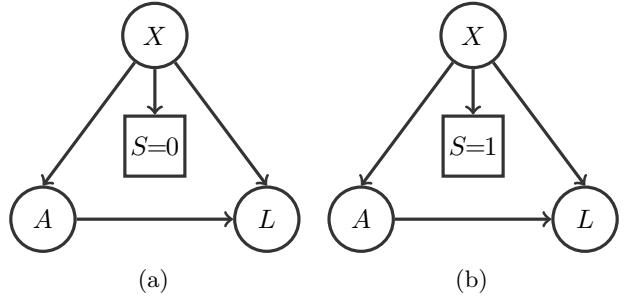


Figure 2: Causal structure of process (a) under policy π as well as (b) trial study. Sampling indicator S distinguishes between the two. For the important case of RCT, assignment of A is not influenced by any covariates so that the path $X \rightarrow A$ is eliminated.

distribution factorizes as

$$p_\pi(X, A, L|S=0) = p(X|S=0) \cdot p_\pi(A|X) \cdot p(L|A, X), \quad (1)$$

where only the policy $p_\pi(A|X)$ is known. Similarly, the trial distribution factorizes as

$$p(X, A, L|S=1) = p(X|S=1) \cdot p(A|X) \cdot p(L|A, X), \quad (2)$$

where only the randomization mechanism $p(A|X)$ is known. In general the characteristics of target and trial populations may differ, that is, $p(X|S=0) \neq p(X|S=1)$.

From the trial distribution (2), we sample m individuals

$$\mathcal{D} = \{(X_i, A_i, L_i)\}_{i=1}^m$$

independently. In addition, we also obtain n independent samples of *covariate-only* data (X_1, X_2, \dots, X_n) from the target population (1). Our aim is to infer the out-of-sample loss L_{n+1} for individual $n+1$ under any policy π . Specifically, we seek a loss limit ℓ_α as a function of $1 - \alpha$, such that $L_{n+1} \leq \ell_\alpha$ holds with probability $1 - \alpha$ as illustrated by the ‘limit curves’ in Figure 1a.

The sampling pattern of individuals is described by $p(S|X)$. This distribution is unknown, but we assume that a model $\hat{p}(S|X)$ is available. This model was fitted using held-out data $\{(X_j, S_j)\}$ employing either the conventional logistic model or any state-of-the-art machine learning models (as exemplified below). It can also be obtained from previous studies. There is, however, no guarantee that $\hat{p}(S|X)$ is calibrated and it may indeed diverge from the unknown sampling pattern. Nevertheless, we want inferences about the out-of-sample loss to be valid also for miscalibrated models. We therefore express the degree of miscalibration in terms of the sampling odds:

$$\frac{1}{\Gamma} \leq \frac{p(S=0|X)}{\underbrace{p(S=1|X)}_{\text{unknown odds}}} \Big/ \frac{\hat{p}(S=0|X)}{\underbrace{\hat{p}(S=1|X)}_{\text{nominal odds}}} \leq \Gamma. \quad (3)$$

That is, the nominal sampling odds can diverge by a factor Γ , where $\Gamma = 1$ implies a perfectly calibrated model. This model includes all sources of errors (selection bias, model misspecification, estimation error).

A limit ℓ_α^Γ provides an *externally valid* inference of L_{n+1} , up to any specified degree of miscalibration Γ , if it satisfies

$$\mathbb{P}_\pi \left\{ L_{n+1} \leq \ell_\alpha^\Gamma(\mathcal{D}) \mid S = 0 \right\} \geq 1 - \alpha, \quad \forall \alpha. \quad (4)$$

The problem we consider is to construct this externally valid limit ℓ_α^Γ . This limit allows us to infer the full loss distribution of a future individual with L_{n+1} under policy π , rather than merely the expected loss $\mathbb{E}_\pi[L]$. Specifically, the tail losses are important in healthcare and other safety critical applications where erroneous inferences could be harmful, and a cautious approach when implementing new policies is needed. By increasing the range of Γ , we certify the validity of the inference under increasingly *credible* assumptions on $\hat{p}(S|X)$ (Manski, 2003). As the model credibility increases, however, the informativeness of the inferences decreases. Since the upper bound on the losses, L_{\max} , is a trivial and uninformative limit, we may define the informativeness of ℓ_α^Γ as

$$\text{Informativeness} = 1 - \inf \{ \alpha : \ell_\alpha^\Gamma(\mathcal{D}) < L_{\max} \}. \quad (5)$$

That is, the right limit of a limit curve, which decreases with the degree of miscalibration. Figure 1a

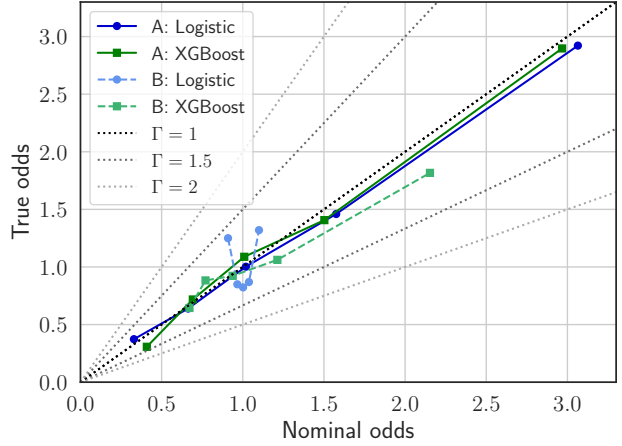


Figure 3: Reliability diagram of the estimated odds against the average nominal odds $\hat{p}(S=0|X)/\hat{p}(S=1|X)$ obtained from logistic and XGBoost models $\hat{p}(S|X)$ for two different target populations A and B. The diagrams provide lower limits for Γ .

shows curves that are valid for miscalibration in the range $\Gamma \in [1, 2]$, where the informativeness is 95% and 85%, respectively. The latter figure means that we can infer an upper bound of the loss for 85% of the target population. The resulting informativeness of a limit curve can therefore guide the specified upper bound of the range of miscalibration in any given problem.

Methods for assessing the calibration of models $\hat{p}(S|X)$ discussed in, e.g., Murphy & Winkler (1977); Naeini et al. (2015); Widmann et al. (2019) can guide the specified lower bound of the range of miscalibration. The nominal odds in (3) can be quantized into several bins and for each bin the unknown odds can be estimated by counting the samples from both the target and trial distributions present. In the case of a well-calibrated model, estimated unknown odds should match the quantized nominal odds for each bin. To assess calibration, this process can be iterated across multiple ranges within the dataset and visualized through a reliability diagram, as exemplified in Figure 3. Further details regarding the experimental setup can be found in Section 5.

3 Background Literature

The problem considered herein is related to the problem of causal inference when combining data from randomized controlled trials and observational studies. Examples of the setting where only covariate data from the observational study is available can be found in Lesko et al. (2016) and Li et al. (2022). For additional examples, refer to the survey by Colnet et al. (2020). Within the broader area of generalizability and trans-

portability, the problem represents the case where the sampling probability depends solely on the covariates X , and is independent of the action and the loss (Pearl & Bareinboim, 2014; Lesko et al., 2017; Degtiar & Rose, 2023). The problem is also related to a broader literature of statistical learning under covariate shifts, see for instance Shimodaira (2000); Sugiyama et al. (2007); Quinonero-Candela et al. (2008); Reddi et al. (2015); Chen et al. (2016).

The most common object of inference in policy evaluation is the expected loss $\mathbb{E}_\pi[L]$ and a popular method for estimating it is inverse probability of sampling weighting (IPSW), which models covariate shifts from trial to target populations. The estimator using RCT-data is defined as

$$V_{\text{IPSW}}^\pi = \frac{1}{n} \sum_{i=1}^m \frac{\widehat{p}(S=0|X_i)}{\widehat{p}(S=1|X_i)} \cdot \frac{p_\pi(A_i|X_i)}{p(A_i)} \cdot L_i. \quad (6)$$

This methodology has been applied in various studies, see for example Cole & Stuart (2010); Stuart et al. (2011); Westreich et al. (2017); Buchanan et al. (2018). It is widely recognized that misspecified logistic models can introduce bias when estimating the weights (Colnet et al., 2020) and more recent works have suggested using flexible models, such as generalized boosted methods (Kern et al., 2016), instead. The counterpart to IPSW, used in off-policy evaluation with observational data, is inverse propensity weighting (IPW). The problem with misspecified logistic models also applies here when estimating the classification probabilities, aka. propensity scores (McCaffrey et al., 2004; Lee et al., 2010). In this case, generalized boosted methods and covariate-balancing methods have shown to be promising alternatives (Setodji et al., 2017; Tu, 2019). The literature on IPSW and IPW is mainly focused on average treatment effect estimation, that is $\mathbb{E}_{\pi_1}[L] - \mathbb{E}_{\pi_0}[L]$ where π_1 and π_0 denote the ‘treat all’ and ‘treat none’ policies, respectively. By contrast, we want to certify the distributional properties of L_{n+1} for any π , even under miscalibration of $\widehat{p}(S|X)$.

Conformal prediction is a distribution-free methodology focused on creating covariate-specific prediction regions that are valid for finite-samples (Vovk et al., 2005; Shafer & Vovk, 2008). The methodology was extended by Tibshirani et al. (2019) to also work for known covariate shifts. Jin et al. (2023) combined the marginal sensitivity methodology developed in Tan (2006) with the conformal prediction for covariate shifts to perform sensitivity analysis of treatment effects in the case of unobserved confounding. Our methodology draws upon techniques in conformal prediction, but instead of providing covariate-specific predictions intervals under a policy π , we are concerned with evaluating *any* π over a target population.

The biased sample selection described by (3) was considered in the context of policy learning by Lei et al. (2023). In contrast to that work, our primary focus is on ensuring the validity of inferences regarding out-of-sample losses, even when dealing with finite training data. We achieve this using a sample-splitting technique.

4 Method

Here we construct a limit $\ell_\alpha^\Gamma(\mathcal{D})$ on the out-of-sample losses under policy π that satisfies (4) for any given specified degree of miscalibration Γ . For this we need to describe the distribution shift from trial to target distribution for all samples, including the $n+1$ sample. We begin by considering the true distribution shift expressed using the ratio

$$\frac{p_\pi(X, A, L|S=0)}{p(X, A, L|S=1)}. \quad (7)$$

Inserting the factorizations (1) and (2) into this ratio shows that specifying the distribution shift requires the unknown (conditional) covariate distribution $p(X|S)$. We can, however, bound (7) using the model of the sampling pattern, $\widehat{p}(S|X)$, as follows:

$$c \cdot \underline{W}^\Gamma \leq \frac{p_\pi(X, A, L|S=0)}{p(X, A, L|S=1)} \leq c \cdot \overline{W}^\Gamma, \quad (8)$$

where

$$\begin{aligned} \underline{W}^\Gamma &= \frac{1}{\Gamma} \cdot \frac{\widehat{p}(S=0|X)}{\widehat{p}(S=1|X)} \cdot \frac{p_\pi(A|X)}{p(A|X)}, \\ \overline{W}^\Gamma &= \Gamma \cdot \frac{\widehat{p}(S=0|X)}{\widehat{p}(S=1|X)} \cdot \frac{p_\pi(A|X)}{p(A|X)}, \end{aligned} \quad (9)$$

and $c = \frac{p(S=1)}{p(S=0)}$ is a constant. To see this, we note that the ratio in (7) can be expressed as

$$c \cdot \frac{p(S=0|X)}{p(S=1|X)} \cdot \frac{p_\pi(A|X)}{p(A|X)},$$

using Bayes’ rule. The bound (8) follows by applying (3). We proceed to show that the factors (9) are sufficient to construct an externally valid limit ℓ_α^Γ for odds divergences up to degree Γ .

To ensure finite-sample guarantees, the trial data is randomly divided into two sets, $\mathcal{D} = \mathcal{D}' \cup \mathcal{D}''$, with respective sample sizes of m' and $m - m'$. The set \mathcal{D}' is used to construct

$$\overline{w}_\beta^\Gamma(\mathcal{D}') = \begin{cases} \overline{W}^\Gamma & [(m'+1)(1-\beta)], \quad (m'+1)(1-\beta) \leq m', \\ \infty & \text{otherwise,} \end{cases} \quad (10)$$

where $\bar{W}_{[\cdot]}^\Gamma$ is the upper limit in (9) evaluated over \mathcal{D}' and ordered $\bar{W}_{[1]}^\Gamma \leq \bar{W}_{[2]}^\Gamma \leq \dots \leq \bar{W}_{[m']}^\Gamma$. We show that (10) upper bounds the ratio (7) for a future sample with probability $1 - \beta$ for any choice of $\beta \in (0, 1)$. The set \mathcal{D}'' is used to construct a stand-in for the unknown cumulative distribution function of the out-of-sample loss:

$$\hat{F}(\ell; \mathcal{D}'', w) = \frac{\sum_{i \in \mathcal{D}''} \underline{W}_i^\Gamma \mathbb{1}(L_i \leq \ell)}{\sum_{i \in \mathcal{D}''} [\underline{W}_i^\Gamma \mathbb{1}(L_i \leq \ell) + \bar{W}_i^\Gamma \mathbb{1}(L_i > \ell)] + w}, \quad (11)$$

where $w > 0$ is a free variable representing the unknown out-of-sample weight \bar{W}_{n+1}^Γ for a future sample. Based on (10) and (11), define $\ell_{\alpha, \beta}^\Gamma$ as the quantile function

$$\ell_{\alpha, \beta}^\Gamma = \inf \left\{ \ell : \hat{F}(\ell; \mathcal{D}'', \bar{w}_\beta^\Gamma(\mathcal{D}')) \geq \frac{1 - \alpha}{1 - \beta} \right\}. \quad (12)$$

This enables us to construct a valid limit on the future loss L_{n+1} for any miscoverage probability $\alpha \in (0, 1)$.

Theorem 4.1. *For any odds miscalibration up to degree Γ ,*

$$\ell_\alpha^\Gamma(\mathcal{D}) = \min_{\beta: 0 < \beta < \alpha} \ell_{\alpha, \beta}^\Gamma, \quad (13)$$

is an externally valid limit on the out-of-sample loss L_{n+1} of policy π . That is, (13) is certified to satisfy (4).

The method seeks the level β for the bound (10) that yields the tightest limit. The proof is presented in the supplementary material and builds on several techniques developed in Vovk et al. (2005); Tibshirani et al. (2019); Jin et al. (2023); Ek et al. (2023).

Algorithm 1 summarizes the implementation of a set of limit curves given a model of the sampling pattern $\hat{p}(S|X)$ and a set of miscalibration degrees $[1, \Gamma_{\max}]$. Note that (10) and (11) are step functions in β respective ℓ . Therefore (12) and (13) can be solved by computing the functions at a grid of points. Calculating (10) and (11) requires the sorting of weights, but the sorting operation is a one-time requirement.

Increasing the degree of miscalibration Γ results in a decrease in \underline{W}^Γ and an increase in \bar{W}^Γ in (9). As weights associated with lower and higher losses decrease and increase, respectively, in (11), the resulting limit $\ell_\alpha^\Gamma(\mathcal{D})$ becomes more conservative.

Remark 1: If the trial population is a small subgroup of the target population (for example in the case of weak overlap), the nominal odds $\frac{\hat{p}(S=0|X)}{\hat{p}(S=1|X)}$ will tend to be high. As this yields a significant weight $\bar{w}_\beta^\Gamma(\mathcal{D}')$, the informativeness (5) of $\ell_\alpha^\Gamma(\mathcal{D})$ diminishes. Nevertheless, the guarantee in (4) holds.

Algorithm 1 A set of limit curves for policy π

input Model $\hat{p}(S|X)$, policy $p_\pi(A|X)$, trial policy $p(A|X)$, a set of miscalibration degrees $\{1, \dots, \Gamma_{\max}\}$ and trial data \mathcal{D} .

output $\{(\Gamma, \alpha, \ell_\alpha^\Gamma)\}$

- 1: Randomly split \mathcal{D} into \mathcal{D}' and \mathcal{D}'' .
- 2: **for** $\Gamma \in \{1, \dots, \Gamma_{\max}\}$ **do**
- 3: **for** $\alpha \in \{0, \dots, 1\}$ **do**
- 4: **for** $\beta \in \{0, \dots, \alpha\}$ **do**
- 5: Compute \bar{w}_β^Γ as in (10).
- 6: Compute $\ell_{\alpha, \beta}^\Gamma$ as in (12).
- 7: **end for**
- 8: Set ℓ_α^Γ to the smallest $\ell_{\alpha, \beta}^\Gamma$.
- 9: Save $(\Gamma, \alpha, \ell_\alpha^\Gamma)$.
- 10: **end for**
- 11: **end for**

Remark 2: The split of \mathcal{D} can be performed in a sample-efficient manner in the case of RCT, where actions are randomized so that $p(A|X) \equiv p(A)$: For the i th sample, (X_i, A_i, L_i) , draw $\tilde{A}_i \sim p_\pi(A|X_i)$. Include sample i in \mathcal{D}'' if $A_i = \tilde{A}_i$, otherwise include it in \mathcal{D}' . This sample splitting method ensures that inferences on the loss are based on actions that match those of the policy.

5 Numerical Experiments

We will use both synthetic and real-world data to illustrate the main concepts of policy evaluation with limit curves $(\alpha, \ell_\alpha^\Gamma)$. As a benchmark, we estimate the quantile using the inverse probability of sampling weighting Colnet et al. (2020)

$$\ell_\alpha(\mathcal{D}) = \inf \{ \ell : \hat{F}_{\text{IPSW}}(\ell; \mathcal{D}) \geq 1 - \alpha \},$$

where

$$\begin{aligned} \hat{F}_{\text{IPSW}}(\ell; \mathcal{D}) &= \\ &1 \sum_{i=1}^m \frac{m}{n} \cdot \frac{\hat{p}(S=0|X_i)}{\hat{p}(S=1|X_i)} \cdot \frac{p_\pi(A_i|X_i)}{p(A_i)} \cdot \mathbb{1}(L_i \leq \ell). \end{aligned}$$

This is similar to the approach in Huang et al. (2021) but adapted to problems involving data from trial and observational studies.

We examine the impact of increasing the credibility of our model assumptions, i.e., by increasing the miscalibration degree Γ , on the informativeness (5) of the limit curve. In addition, for the simulated data, we also assess the miscoverage gap of the curves

$$\text{Miscoverage gap} = \alpha - \mathbb{P}_\pi\{L_{n+1} > \ell_\alpha(\mathcal{D}) | S=0\},$$

where a negative gap indicates an invalid limit.

Table 1: Means and variances of covariate distribution $p(X|S)$ in (14).

Population	$\mu_{0,S}$	$\mu_{1,S}$	$\sigma_{0,S}^2$	$\sigma_{1,S}^2$
A ($S = 0$)	0.5	0.5	1.0	1.0
B ($S = 0$)	0.0	0.0	1.5	1.5
C ($S = 0$)	0.5	0.5	1.5	1.5
Trial ($S = 1$)	0.0	0.0	1.0	1.0

5.1 Illustrations using synthetic data

We consider target and trial populations of individuals with two-dimensional covariates, distributed as follows:

$$X|S = \begin{bmatrix} X_{0,S} \\ X_{1,S} \end{bmatrix} \sim \mathcal{N} \left(\begin{bmatrix} \mu_{0,S} \\ \mu_{1,S} \end{bmatrix}, \begin{bmatrix} \sigma_{0,S}^2 & 0 \\ 0 & \sigma_{1,S}^2 \end{bmatrix} \right), \quad (14)$$

where the parameters are given in Table 1. The distributions for populations A, B, C and Trial are taken to be unknown.

The actions are binary $A \in \{0, 1\}$ and corresponds to ‘do not treat’ versus ‘treat’. We begin by evaluating the ‘treat all’ policy, i.e.,

$$p_{\pi_1}(A = 1|X) = 1.$$

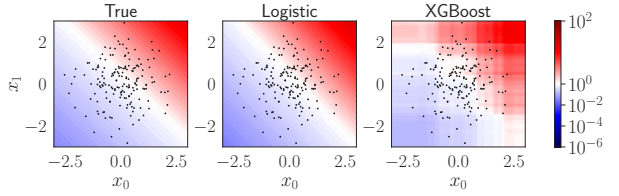
The trial is an RCT with equal probability of assignment, i.e., $p(A) \equiv 0.5$. The unknown conditional loss distribution is given by

$$L|(A, X) \sim \mathcal{N}(A \cdot X_0^2 + X_1 + 2 \cdot (1 - A), 1).$$

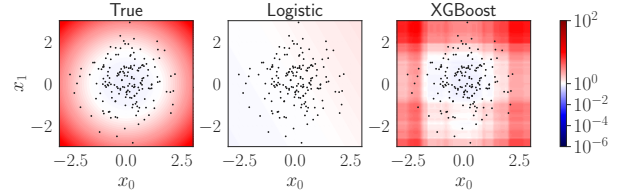
The sampling probability $p(S|X)$ is treated as unknown. To illustrate the generality of the proposed methodology, we consider two different fitted models $\hat{p}(S|X)$: a logistic model, which is conventionally used in the causal inference literature (Westreich et al., 2017), and the more flexible tree-based ensemble model trained by XGBoost (Chen & Guestrin, 2016). The complete set of hyperparameters used is provided in the supplementary material.

For the observational data $(X_i)_{i=1}^n$, we drew $n = 2000$ samples. For the trial data we drew 1000 samples: $m = 500$ samples $((X_i, A_i, L_i))_{i=1}^m$ were used to compute the limit curves, and the remaining 500 samples were used to train $\hat{p}(S|X)$.

Figure 4a compares nominal sampling odds obtained from the fitted models with the unknown odds $p(S = 0|X)/p(S = 1|X)$ for target population A. In this case, the logistic model happens to be well-specified so that the learned odds approximate the true ones well. The more flexible XGBoost model also provide visually similar odds, albeit less accurate. By contrast, Figure 4b repeats the same exercise for target population B. Here the logistic model is misspecified and severely miscalibrated while the XGBoost model continues to provide



(a) Sampling odds for target population A.



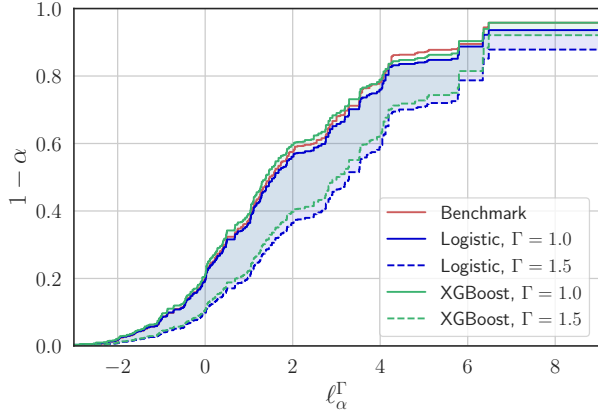
(b) Sampling odds for target population B.

Figure 4: True sampling odds $p(S = 0|X)/p(S = 1|X)$ compared with nominal odds obtained from logistic and XGBoost models $\hat{p}(S|X)$. The dots are a random subsample of the trial samples.

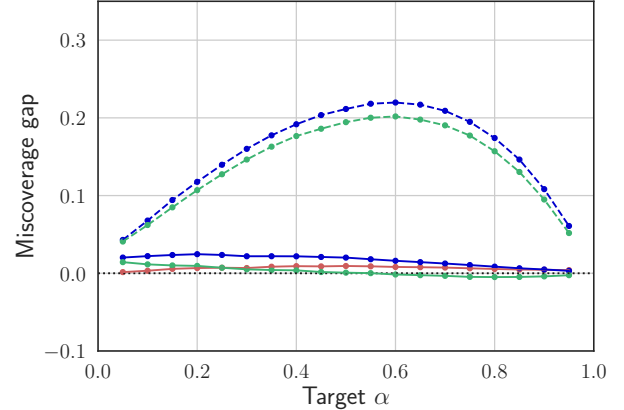
visually similar odds. A reliability diagram is used in Figure 3 for a quantitative metric for the divergence of the odds for the same scenarios. The reliability diagram uses 5 bins and shows the observed odds against the average predicted nominal odds $\hat{p}(S = 0|X)/\hat{p}(S = 1|X)$ for respective model. For target population A, both models are close to the diagonal and a degree of misspecification Γ close to 1 is reasonable. For population B and the (misspecified) logistic model we see that a larger lower bound, $\Gamma \approx 1.5$, is appropriate, while for XGBoost model $\Gamma \approx 1$ is still reasonable.

We then evaluate the out-of-sample loss of the ‘treat all’ policy π_1 using the limit curve for the benchmark and the limit curves for the proposed method. Figure 5a shows the evaluation with respect to population A, where all the limit curves are similar. The curves for the proposed method also illustrate increasing the credibility of the models results in less informative inferences. However, their informativeness stays above 90% for odds miscalibration degrees $\Gamma \in [1, 1.5]$. Since the data is simulated, we evaluate the miscoverage gap of the curves in Figure 5b. The gap is estimated using 1000 independent runs and for each run drawing 1000 independent new samples $(X_{n+1}, A_{n+1}, L_{n+1})$. We see that the benchmark and the well-specified logistic model yields a valid and tight limit curve for $\Gamma = 1$, whereas the XGBoost model has only a slight negative miscoverage gap. As the degree of miscalibration Γ increases to 1.5, the limit curves exhibit positive miscoverage gaps, where XGBoost results in slightly less conservative inferences than the logistic model does.

We contrast the above results with the evaluation of π_1 when applied to population B as shown in Figure 6a.



(a)



(b)

Figure 5: Evaluating ‘treat all’ policy π_1 for target population A with degrees of miscalibration $\Gamma \in [1, 1.5]$.

The benchmark and the logistic model result in a similar limit curve, while XGBoost infer higher losses of π_1 . Figure 6b shows that the benchmark and the (misspecified) logistic model when assuming $\Gamma = 1$ now yields negative miscoverage gaps, whereas XGBoost yields a valid and tight limit curve. Again, when the degree of miscalibration increases to 1.5 both proposed models yield positive gaps. Our contrast between populations A and B shows that the use of more adaptable and, thus potentially better calibrated, models $\hat{p}(S|X)$ can be advantageous over the conventional logistic or generalized linear models.

We now turn to comparing the ‘treat all’ policy with a ‘treat none’ policy, i.e., $p_{\pi_0}(A = 0|X) = 1$, for population A. Their expected losses are estimated using (6) as $V_{\text{IPSW}}^{\pi_0} = 2.73$ and $V_{\text{IPSW}}^{\pi_1} = 1.85$, respectively. This evaluation suggests that π_1 is preferable to π_0 . However, the limit curves presented in Figure 7 provide a more detailed picture in terms of out-of-sample losses: the tail losses certified for the ‘treat all’ policy π_0 are lower than those certified for π_1 . This illustrates the cautionary principle built into the policy evaluations.

The evaluation of π_1 with respect to population C for the logistic model of $\hat{p}(S|X)$ is shown in Figure 1. More results for population C and results for additional populations are available in the supplementary material.

5.2 Evaluating seafood consumption policies

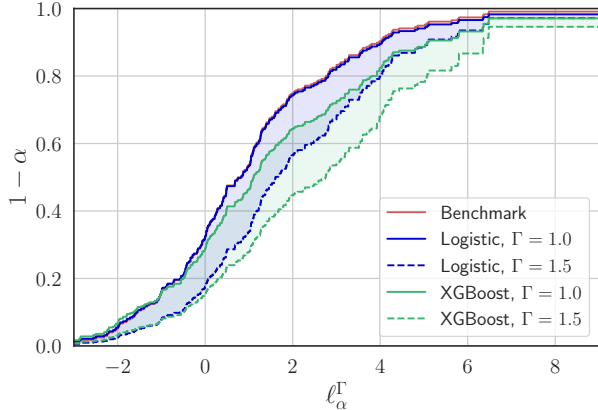
To illustrate the application of policy evaluation with real data, we study the impact of seafood consumption on blood mercury levels with data from the 2013-2014 National Health and Nutrition Examination Survey (NHANES). Following Zhao et al. (2019), each individual’s data includes eight covariates, denoted X , encompassing gender, age, income, the presence or absence of

income information, race, education, smoking history, and the number of cigarettes smoked in the last month. We excluded one individual due to missing education data and seven individuals with incomplete smoking data. We impute the median income for 175 individuals with no income information. After the preprocessing, our data set comprises 1107 individuals. The data is then split into observational data \mathcal{D}_0 and trial data \mathcal{D}_1 with a probability $p(S = 1|X_{\text{age}} \leq 35) = 0.8$ respective $p(S = 1|X_{\text{age}} > 35) = 0.2$ resulting in 637 samples in the observational data and 470 samples in the trial data. The action A describes individual fish or shellfish consumption, categorizing an individual as having either low (≤ 1 serving in the past month) or high (> 12 servings in the past month) consumption. The loss L represents the total concentration of blood mercury (measured in $\mu\text{g}/\text{L}$).

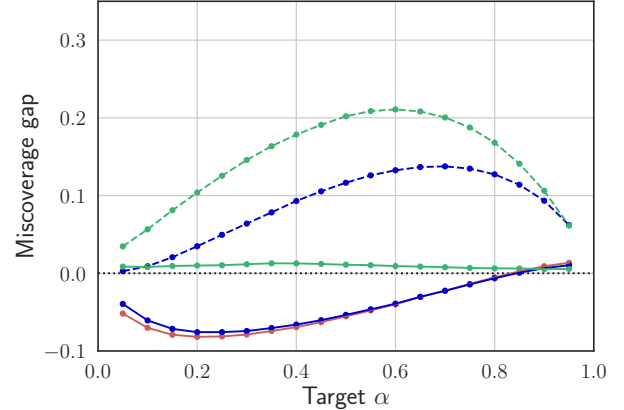
To generate counterfactual actions and losses, we consider a balanced RCT so that $p(A) \equiv 0.5$ and learn a model of $p(L|A, X)$ from the data using gradient boosting (Freund & Schapire, 1997; Friedman et al., 2000). Thus during training, the trial data consists of samples (X_i, A_i, L_i) whereas the observational data only contains X .

A reliability diagram, as shown in Figure 8, compares a logistic model and a XGBoost-trained model. The XGBoost model is closer to the diagonal, and is therefore chosen and a Γ close to 1 is a reasonable lower limit.

In Figure 9 we compare the limit curve for a policy π_0 corresponding to low ($A \equiv 0$) seafood consumption with the limit curve for a policy π_1 corresponding to high ($A \equiv 1$) seafood consumption. We use an XGBoost-trained model $\hat{p}(S|X)$. For reference, a mercury level of 8 $\mu\text{g}/\text{L}$ is guidance limit for women of child-bearing age. We see that under a low consumption policy a lower mercury level can be certified for miscalibrated odds



(a)



(b)

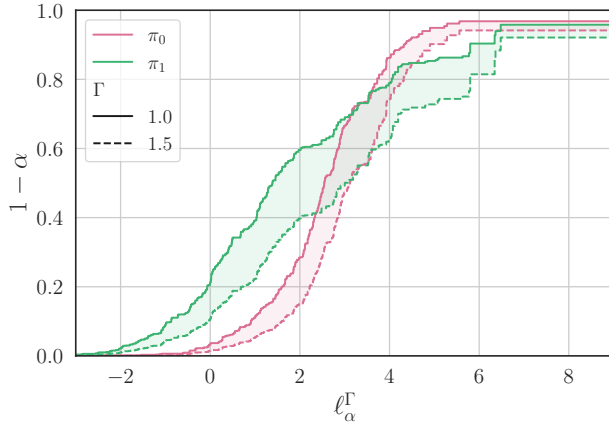
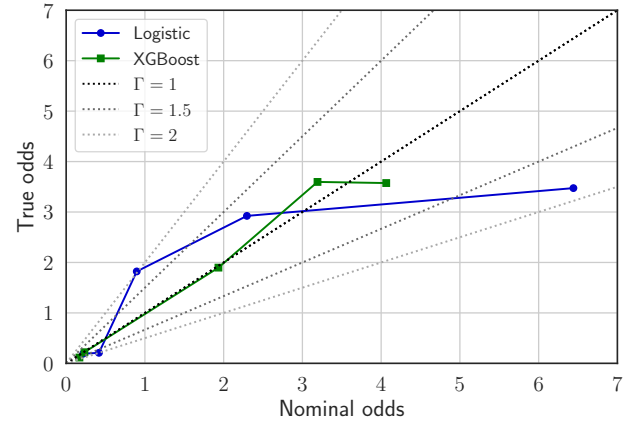
Figure 6: Evaluating ‘treat all’ policy π_1 for target population B with degrees of miscalibration $\Gamma \in [1, 1.5]$.Figure 7: Limit curves for π_0 and π_1 for target population A certified for $\Gamma \in [1, 1.5]$.

Figure 8: Reliability diagram of the observed odds against the average predicted nominal odds obtained from logistic and XGBoost-trained models.

$\Gamma \in [1, 2]$. In this case, we can infer a 90% probability that the out-of-sample mercury level falls below the reference value of 8 $\mu\text{g/L}$.

6 Discussion

We have proposed a method for establishing externally valid policy evaluation based on experimental results from trial studies. The method is nonparametric, making no assumptions on the distributional forms of the data. Using covariate-only data from a target population, it takes into account possible covariate shifts between target and trial populations, and certifies valid finite-sample inferences of the out-of-sample loss L_{n+1} , up to any specified degree of model miscalibration.

Conventional policy evaluation methods focus on $\mathbb{E}_\pi[L]$ and can easily introduce a bias without the user’s awareness, particularly when the model of the sampling pat-

tern $\hat{p}(S|X)$ is misspecified. Lacking any control for miscalibration undermines the possibility to establish external validity. In safety-critical applications, making invalid inferences about a decision policy can be potentially harmful. Hence, adhering to the cautionary principle of “above all, do no harm” is important. The proposed method is designed with this principle in mind, and the limit curve represents the worst-case scenario for the selected degree of miscalibration Γ .

We also exemplify how the reliability diagram technique can be used to assess the divergences of the model odds and facilitate a more systematic guidance on both model selection and on the specification of the odds miscalibration degree Γ in a given problem.

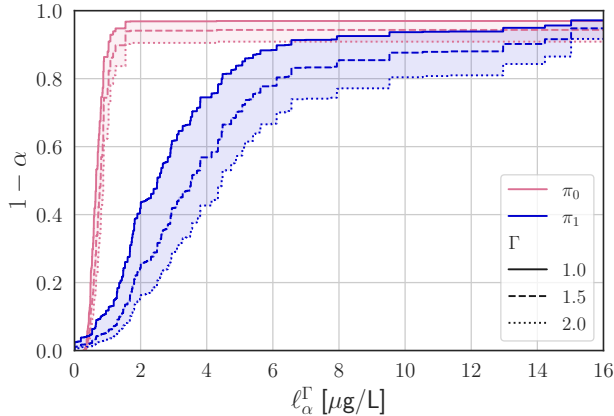


Figure 9: Inferred blood mercury levels [$\mu\text{g/L}$] in a target population under ‘high’ and ‘low’ seafood consumption (π_1 and π_0 , respectively). Limit curves for degrees of odds miscalibration $\Gamma \in [1, 2]$.

7 Broader Impact

The method we propose is designed for safety-critical applications, such as clinical decision support, with the cautionary principle in mind. We believe that it offers a valuable tool for policy evaluation in such scenarios. Our approach focuses on limit curves, coupled with a statistical guarantee, for a more detailed understanding of the out-of-sample loss. This facilitates a fairer evaluation by bringing attention to sensitive covariates in the tails. However, it remains important to be aware of biases, and it might be necessary to address them separately to prevent their replication.

References

Buchanan, A. L., Hudgens, M. G., Cole, S. R., Mollan, K. R., Sax, P. E., Daar, E. S., Adimora, A. A., Eron, J. J., and Mugavero, M. J. Generalizing evidence from randomized trials using inverse probability of sampling weights. *Journal of the Royal Statistical Society Series A: Statistics in Society*, 181(4):1193–1209, 2018.

Campbell, D. and Stanley, J. *Experimental and Quasi-experimental Designs for Research*. R. McNally College Publishing Company, 1963.

Chen, T. and Guestrin, C. Xgboost: A scalable tree boosting system. In *Proceedings of the 22nd ACM SIGKDD international conference on knowledge discovery and data mining*, pp. 785–794, 2016.

Chen, X., Monfort, M., Liu, A., and Ziebart, B. D. Robust covariate shift regression. In *Artificial Intelligence and Statistics*, pp. 1270–1279. PMLR, 2016.

Cole, S. R. and Stuart, E. A. Generalizing evidence from randomized clinical trials to target populations: the actg 320 trial. *American journal of epidemiology*, 172(1):107–115, 2010.

Colnet, B., Mayer, I., Chen, G., Dieng, A., Li, R., Varoquaux, G., Vert, J.-P., Josse, J., and Yang, S. Causal inference methods for combining randomized trials and observational studies: a review. *arXiv preprint arXiv:2011.08047*, 2020.

Degtyar, I. and Rose, S. A review of generalizability and transportability. *Annual Review of Statistics and Its Application*, 10:501–524, 2023.

Ek, S., Zachariah, D., Johansson, F. D., and Stoica, P. Off-policy evaluation with out-of-sample guarantees. *Transactions on Machine Learning Research*, 2023.

Freund, Y. and Schapire, R. E. A decision-theoretic generalization of on-line learning and an application to boosting. *Journal of computer and system sciences*, 55(1):119–139, 1997.

Friedman, J., Hastie, T., and Tibshirani, R. Additive logistic regression: a statistical view of boosting (with discussion and a rejoinder by the authors). *The annals of statistics*, 28(2):337–407, 2000.

Huang, A., Leqi, L., Lipton, Z., and Azizzadenesheli, K. Off-policy risk assessment in contextual bandits. *Advances in Neural Information Processing Systems*, 34:23714–23726, 2021.

Jin, Y., Ren, Z., and Candès, E. J. Sensitivity analysis of individual treatment effects: A robust conformal inference approach. *Proceedings of the National Academy of Sciences*, 120(6), 2023.

Kern, H. L., Stuart, E. A., Hill, J., and Green, D. P. Assessing methods for generalizing experimental impact estimates to target populations. *Journal of research on educational effectiveness*, 9(1):103–127, 2016.

Kosorok, M. R. and Laber, E. B. Precision medicine. *Annual review of statistics and its application*, 6:263–286, 2019.

Lee, B. K., Lessler, J., and Stuart, E. A. Improving propensity score weighting using machine learning. *Statistics in medicine*, 29(3):337–346, 2010.

Lei, J., G’Sell, M., Rinaldo, A., Tibshirani, R. J., and Wasserman, L. Distribution-free predictive inference for regression. *Journal of the American Statistical Association*, 113(523):1094–1111, 2018.

Lei, L., Sahoo, R., and Wager, S. Policy learning under biased sample selection. *arXiv preprint arXiv:2304.11735*, 2023.

Lesko, C. R., Cole, S. R., Hall, H. I., Westreich, D., Miller, W. C., Eron, J. J., Li, J., Mugavero, M. J., and Investigators, C. The effect of antiretroviral therapy on all-cause mortality, generalized to persons diagnosed with hiv in the usa, 2009–11. *International journal of epidemiology*, 45(1):140–150, 2016.

Lesko, C. R., Buchanan, A. L., Westreich, D., Edwards, J. K., Hudgens, M. G., and Cole, S. R. Generalizing study results: a potential outcomes perspective. *Epidemiology (Cambridge, Mass.)*, 28(4):553, 2017.

Li, F., Buchanan, A. L., and Cole, S. R. Generalizing trial evidence to target populations in non-nested designs: Applications to aids clinical trials. *Journal of the Royal Statistical Society Series C: Applied Statistics*, 71(3):669–697, 2022.

Manski, C. F. Identification problems in the social sciences and everyday life. *Southern Economic Journal*, 70(1):11–21, 2003.

Manski, C. F. *Identification for prediction and decision*. Harvard University Press, 2007.

McCaffrey, D. F., Ridgeway, G., and Morral, A. R. Propensity score estimation with boosted regression for evaluating causal effects in observational studies. *Psychological methods*, 9(4):403, 2004.

Murphy, A. H. and Winkler, R. L. Reliability of subjective probability forecasts of precipitation and temperature. *Journal of the Royal Statistical Society Series C: Applied Statistics*, 26(1):41–47, 1977.

Naeini, M. P., Cooper, G., and Hauskrecht, M. Obtaining well calibrated probabilities using bayesian binning. *Proceedings of the AAAI conference on artificial intelligence*, 29(1), 2015.

Pearl, J. and Bareinboim, E. External Validity: From Do-Calculus to Transportability Across Populations. *Statistical Science*, 29(4):579 – 595, 2014. doi: 10.1214/14-STS486.

Peters, J., Janzing, D., and Schölkopf, B. *Elements of causal inference: foundations and learning algorithms*. The MIT Press, 2017.

Qian, M. and Murphy, S. A. Performance guarantees for individualized treatment rules. *Annals of statistics*, 39(2):1180, 2011.

Quinonero-Candela, J., Sugiyama, M., Schwaighofer, A., and Lawrence, N. D. *Dataset shift in machine learning*. Mit Press, 2008.

Reddi, S., Poczos, B., and Smola, A. Doubly robust covariate shift correction. *Proceedings of the AAAI Conference on Artificial Intelligence*, 29(1), 2015.

Setodji, C. M., McCaffrey, D. F., Burgette, L. F., Almirall, D., and Griffin, B. A. The right tool for the job: Choosing between covariate balancing and generalized boosted model propensity scores. *Epidemiology (Cambridge, Mass.)*, 28(6):802, 2017.

Shafer, G. and Vovk, V. A tutorial on conformal prediction. *Journal of Machine Learning Research*, 9(3), 2008.

Shimodaira, H. Improving predictive inference under covariate shift by weighting the log-likelihood function. *Journal of statistical planning and inference*, 90(2):227–244, 2000.

Smith, C. M. Origin and uses of primum non nocere—above all, do no harm! *The Journal of Clinical Pharmacology*, 45(4):371–377, 2005.

Stuart, E. A., Cole, S. R., Bradshaw, C. P., and Leaf, P. J. The use of propensity scores to assess the generalizability of results from randomized trials. *Journal of the Royal Statistical Society Series A: Statistics in Society*, 174(2):369–386, 2011.

Sugiyama, M., Nakajima, S., Kashima, H., Buenau, P., and Kawanabe, M. Direct importance estimation with model selection and its application to covariate shift adaptation. *Advances in neural information processing systems*, 20, 2007.

Tan, Z. A distributional approach for causal inference using propensity scores. *Journal of the American Statistical Association*, 101(476):1619–1637, 2006.

Tibshirani, R. J., Foygel Barber, R., Candes, E., and Ramdas, A. Conformal prediction under covariate shift. In *Advances in Neural Information Processing Systems*, volume 32. Curran Associates, Inc., 2019.

Tu, C. Comparison of various machine learning algorithms for estimating generalized propensity score. *Journal of Statistical Computation and Simulation*, 89(4):708–719, 2019.

Vovk, V., Gammerman, A., and Shafer, G. *Algorithmic learning in a random world*. Springer Science & Business Media, 2005.

Wang, L., Zhou, Y., Song, R., and Sherwood, B. Quantile-optimal treatment regimes. *Journal of the American Statistical Association*, 113(523):1243–1254, 2018.

Westreich, D. *Epidemiology by Design: A Causal Approach to the Health Sciences*. Oxford University Press, Incorporated, 2019. ISBN 9780190665760.

Westreich, D., Edwards, J. K., Lesko, C. R., Stuart, E., and Cole, S. R. Transportability of trial results using inverse odds of sampling weights. *American journal of epidemiology*, 186(8):1010–1014, 2017.

Widmann, D., Lindsten, F., and Zachariah, D. Calibration tests in multi-class classification: A unifying framework. *Advances in neural information processing systems*, 32, 2019.

Zhao, Q., Small, D. S., and Bhattacharya, B. B. Sensitivity analysis for inverse probability weighting estimators via the percentile bootstrap. *Journal of the Royal Statistical Society: Series B (Statistical Methodology)*, 81(4):735–761, 2019.

Zhao, Y., Zeng, D., Rush, A. J., and Kosorok, M. R. Estimating individualized treatment rules using outcome weighted learning. *Journal of the American Statistical Association*, 107(499):1106–1118, 2012.

A Proof

The proof technique presented here builds upon several results established in Vovk et al. (2005); Tibshirani et al. (2019); Jin et al. (2023); Ek et al. (2023).

Use (12) to construct the limit

$$\ell_\alpha^\Gamma(\mathcal{D}) = \inf \left\{ \ell : \widehat{F}(\ell; \mathcal{D}'', \bar{w}_\beta^\Gamma(\mathcal{D}')) \geq \frac{1-\alpha}{1-\beta} \right\}, \quad (15)$$

for any $0 < \beta < \alpha$, where $\bar{w}_\beta^\Gamma(\mathcal{D}')$ is defined in (10). We want to lower bound the probability of $L_{n+1} \leq \ell_\alpha^\Gamma(\mathcal{D})$. First, note that

$$\begin{aligned} \mathbb{P}\{L_{n+1} \leq \ell_\alpha^\Gamma(\mathcal{D})\} &= \mathbb{P}\{L_{n+1} \leq \ell_\alpha^\Gamma(\mathcal{D}) \mid \bar{W}_{n+1}^\Gamma \leq \bar{w}_\beta^\Gamma(\mathcal{D}')\} \mathbb{P}\{\bar{W}_{n+1}^\Gamma \leq \bar{w}_\beta^\Gamma(\mathcal{D}')\} \\ &\quad + \mathbb{P}\{L_{n+1} \leq \ell_\alpha^\Gamma(\mathcal{D}) \mid \bar{W}_{n+1}^\Gamma > \bar{w}_\beta^\Gamma(\mathcal{D}')\} \mathbb{P}\{\bar{W}_{n+1}^\Gamma > \bar{w}_\beta^\Gamma(\mathcal{D}')\}, \end{aligned}$$

from the law of total probability. The second term is a lower bounded by zero, and we have

$$\mathbb{P}\{L_{n+1} \leq \ell_\alpha^\Gamma(\mathcal{D})\} \geq \mathbb{P}\{L_{n+1} \leq \ell_\alpha^\Gamma(\mathcal{D}) \mid \bar{W}_{n+1}^\Gamma \leq \bar{w}_\beta^\Gamma(\mathcal{D}')\} \mathbb{P}\{\bar{W}_{n+1}^\Gamma \leq \bar{w}_\beta^\Gamma(\mathcal{D}')\}. \quad (16)$$

Let us focus on the second factor in (16). From the construction in (10) the probability of $\bar{W}_{n+1}^\Gamma \leq \bar{w}_\beta^\Gamma(\mathcal{D}')$ is lower bounded by

$$\mathbb{P}\{\bar{W}_{n+1}^\Gamma \leq \bar{w}_\beta^\Gamma(\mathcal{D}')\} \geq 1 - \beta, \quad (17)$$

see Vovk et al. (2005); Lei et al. (2018).

We now proceed to bound the first factor in (16), i.e., $\mathbb{P}\{L_{n+1} \leq \ell_\alpha^\Gamma(\mathcal{D}) \mid \bar{W}_{n+1}^\Gamma \leq \bar{w}_\beta^\Gamma(\mathcal{D}')\}$. Define the following limit

$$\ell_\alpha^\Gamma(\mathcal{D}'', \bar{W}_{n+1}^\Gamma) = \inf \left\{ \ell : \widehat{F}(\ell; \mathcal{D}'', \bar{W}_{n+1}^\Gamma) \geq \frac{1-\alpha}{1-\beta} \right\}, \quad (18)$$

where $\bar{W}_{n+1}^\Gamma \geq W_{n+1}$ is given in (8). Comparing this limit with the one defined in (15), we see that

$$\begin{aligned} \mathbb{P}\{L_{n+1} \leq \ell_\alpha^\Gamma(\mathcal{D}) \mid \bar{W}_{n+1}^\Gamma \leq \bar{w}_\beta^\Gamma(\mathcal{D}')\} &\geq \mathbb{P}\{L_{n+1} \leq \ell_\alpha^\Gamma(\mathcal{D}'', \bar{W}_{n+1}^\Gamma) \mid \bar{W}_{n+1}^\Gamma \leq \bar{w}_\beta^\Gamma(\mathcal{D}')\} \\ &= \mathbb{P}\{L_{n+1} \leq \ell_\alpha^\Gamma(\mathcal{D}'', \bar{W}_{n+1}^\Gamma)\}, \end{aligned}$$

whenever $\bar{W}_{n+1}^\Gamma \leq \bar{w}_\beta^\Gamma(\mathcal{D}')$. The second line follows from using sample splitting, which ensures that $L_{n+1} \leq \ell_\alpha^\Gamma(\mathcal{D}'', \bar{W}_{n+1}^\Gamma)$ and $\bar{W}_{n+1}^\Gamma \leq \bar{w}_\beta^\Gamma(\mathcal{D}')$ are independent events.

To lower bound $\mathbb{P}\{L_{n+1} \leq \ell_\alpha^\Gamma(\mathcal{D}'', \bar{W}_{n+1}^\Gamma)\}$, we will make use of the following inequality,

$$\mathbb{E} \left[\widehat{F}(\ell_\alpha^\Gamma; \mathcal{D}'', \bar{W}_{n+1}^\Gamma) \right] = \mathbb{E} \left[\frac{\sum_{i \in \mathcal{D}''} \bar{W}_i^\Gamma \mathbf{1}(L_i \leq \ell_\alpha^\Gamma)}{\sum_{i \in \mathcal{D}''} [\bar{W}_i^\Gamma \mathbf{1}(L_i \leq \ell_\alpha^\Gamma) + \bar{W}_i^\Gamma \mathbf{1}(L_i > \ell_\alpha^\Gamma)] + \bar{W}_{n+1}^\Gamma} \right] \geq \frac{1-\alpha}{1-\beta}, \quad (19)$$

that holds by construction.

First, define \mathcal{S}_+ as an unordered set of the following elements

$$((X_{m'_0+1}, A_{m'_0+1}, L_{m'_0+1}), \dots, (X_m, A_m, L_m), (X_{n+1}, A_{n+1}, L_{n+1})).$$

From Tibshirani et al. (2019) we have that the out-of-sample loss L_{n+1} has the (conditional) cdf

$$\mathbb{P}\{L_{n+1} \leq \ell \mid \mathcal{S}_+\} = \sum_{i \in \mathcal{S}_+} p_i \mathbf{1}(\ell_i \leq \ell) = \frac{\sum_{i \in \mathcal{S}_+} w_i \mathbf{1}(L_i \leq \ell)}{\sum_{i \in \mathcal{S}_+} w_i}. \quad (20)$$

Next, we build on the proof method used in Jin et al. (2023, thm. 2.2). Use the limit $\ell_\alpha^\Gamma(\mathcal{D}'', \bar{W}_{n+1}^\Gamma)$ from (18) in (20) and apply the law of total expectation to perform marginalization over \mathcal{S}_+

$$\begin{aligned}\mathbb{P}\{L_{n+1} \leq \ell_\alpha^\Gamma(\mathcal{D}'', \bar{W}_{n+1}^\Gamma)\} &= \mathbb{E}[\mathbb{P}\{L_{n+1} \leq \ell_\alpha^\Gamma(\mathcal{D}'', \bar{W}_{n+1}^\Gamma) \mid \mathcal{S}_+\}] \\ &= \mathbb{E}\left[\frac{\sum_{i \in \mathcal{S}_+} W_i \mathbb{1}(L_i \leq \ell_\alpha^\Gamma(\mathcal{D}'', \bar{W}_{n+1}^\Gamma))}{\sum_{i \in \mathcal{S}_+} W_i}\right].\end{aligned}\quad (21)$$

We can now proceed to establish a lower bound for this probability. Combining (19) and (21), we have that

$$\begin{aligned}\mathbb{P}\{L_{n+1} \leq \ell_\alpha^\Gamma(\mathcal{D}'', \bar{W}_{n+1}^\Gamma)\} &- \frac{1-\alpha}{1-\beta} \\ &\geq \mathbb{E}\left[\frac{\sum_{i \in \mathcal{S}_+} W_i \mathbb{1}(L_i \leq \ell_\alpha^\Gamma)}{\sum_{i \in \mathcal{S}_+} W_i}\right] - \mathbb{E}\left[\frac{\sum_{i \in \mathcal{D}''} \underline{W}_i^\Gamma \mathbb{1}(L_i \leq \ell_\alpha^\Gamma)}{\sum_{i \in \mathcal{D}''} [\underline{W}_i^\Gamma \mathbb{1}(L_i \leq \ell_\alpha^\Gamma) + \underline{W}_i^\Gamma \mathbb{1}(L_i > \ell_\alpha^\Gamma)] + \bar{W}_{n+1}^\Gamma}\right] \\ &= \mathbb{E}\left[\frac{(*)}{\left[\sum_{i \in \mathcal{S}_+} W_i\right] \left[\sum_{i \in \mathcal{D}''} [\underline{W}_i^\Gamma \mathbb{1}(L_i \leq \ell_\alpha^\Gamma) + \underline{W}_i^\Gamma \mathbb{1}(L_i > \ell_\alpha^\Gamma)] + \bar{W}_{n+1}^\Gamma\right]}\right],\end{aligned}$$

where

$$\begin{aligned}(*) &= \left[\sum_{i \in \mathcal{S}_+} W_i \mathbb{1}(L_i \leq \ell_\alpha^\Gamma)\right] \left[\sum_{i \in \mathcal{D}''} \underline{W}_i^\Gamma \mathbb{1}(L_i > \ell_\alpha^\Gamma) + \bar{W}_{n+1}^\Gamma\right] - \left[\sum_{i \in \mathcal{D}''} \underline{W}_i^\Gamma \mathbb{1}(L_i \leq \ell_\alpha^\Gamma)\right] \left[\sum_{i \in \mathcal{S}_+} W_i \mathbb{1}(L_i > \ell_\alpha^\Gamma)\right] \\ &\geq \left[\sum_{i \in \mathcal{D}''} W_i \mathbb{1}(L_i \leq \ell_\alpha^\Gamma)\right] \left[\sum_{i \in \mathcal{D}''} W_i \mathbb{1}(L_i > \ell_\alpha^\Gamma) + W_{n+1}\right] - \left[\sum_{i \in \mathcal{D}''} W_i \mathbb{1}(L_i \leq \ell_\alpha^\Gamma)\right] \left[\sum_{i \in \mathcal{D}''} W_i \mathbb{1}(L_i > \ell_\alpha^\Gamma) + W_{n+1}\right] \\ &= 0.\end{aligned}$$

We use the bounds provided in (8) to derive the inequality. Hence, we arrive at a valid limit

$$\mathbb{P}\{L_{n+1} \leq \ell_\alpha^\Gamma(\mathcal{D}'', \bar{W}_{n+1}^\Gamma)\} \geq \frac{1-\alpha}{1-\beta}. \quad (22)$$

Finally combine (17) and (22) to get

$$\begin{aligned}\mathbb{P}\{L_{n+1} \leq \ell_\alpha^\Gamma(\mathcal{D})\} &\geq \mathbb{P}\{L_{n+1} \leq \ell_\alpha^\Gamma(\mathcal{D}'', \bar{W}_{n+1}^\Gamma)\} \mathbb{P}\{\bar{W}_{n+1}^\Gamma \leq \bar{w}_\beta^\Gamma(\mathcal{D}')\} \\ &\geq \frac{1-\alpha}{1-\beta} (1-\beta) \\ &= 1-\alpha.\end{aligned}\quad (23)$$

We choose β as in (13) to get the tightest limit. Note that in this context, \mathbb{P} represents the probability over samples drawn from both $p(X, A, L|S=1)$ and $p_\pi(X, A, L|S=0)$. As L_{n+1} is drawn from $p_\pi(X, A, L|S=0)$, we can express (23) as shown in (4) for the sake of notational clarity.

B Numerical Experiments

Additional information of the numerical experiments outlined in Section 5 can be found in this supplementary material. All experiments were conducted using Version 1.7 of the Python implementation of XGBoost. A comprehensive list of hyperparameters is available in Table 2 for the synthetic case and Table 3 for the NHANES case. The hyperparameters were selected through a random search involving 200 runs, employing 5-fold cross-validation with the F1 score as the optimization metric.

Table 2: Hyperparameters used for XGBoost in Section 5.1.

Parameter	Value
<code>n_estimators</code>	100
<code>max_depth</code>	2
<code>learning_rate</code>	0.05
<code>objective</code>	<code>binary:logistic</code>
<code>min_child_weight</code>	1
<code>subsample</code>	0.6
<code>colsample_bytree</code>	0.8
<code>colsample_bylevel</code>	0.4
<code>scale_pos_weight</code>	$n_{s=0}/n_{s=1}$

Table 3: Hyperparameters used for XGBoost in Section 5.2.

Parameter	Value
<code>n_estimators</code>	50
<code>max_depth</code>	1
<code>learning_rate</code>	0.2
<code>objective</code>	<code>binary:logistic</code>
<code>min_child_weight</code>	1
<code>subsample</code>	0.4
<code>colsample_bytree</code>	0.7
<code>colsample_bylevel</code>	0.8
<code>scale_pos_weight</code>	$n_{s=0}/n_{s=1}$

B.1 Reliability diagram

We use the reliability diagram technique to guide the lower bound of the range of miscalibration. We therefore need an estimate of the unknown odds

$$\frac{p(S = 0|X)}{p(S = 1|X)},$$

to be compare against the nominal odds

$$\frac{\widehat{p}(S = 0|X)}{\widehat{p}(S = 1|X)}.$$

Using (3), we have that

$$\frac{1}{\Gamma} \cdot \widehat{\text{odds}}(X) \leq \text{odds}(X) \leq \Gamma \cdot \widehat{\text{odds}}(X).$$

Take the expectation with respect to X , conditional on the nominal odds is in a specified interval (or bin) I , so that:

$$\frac{1}{\Gamma} \cdot \mathbb{E}[\widehat{\text{odds}}(X) | \widehat{\text{odds}}(X) \in I] \leq \mathbb{E}[\text{odds}(X) | \widehat{\text{odds}}(X) \in I] \leq \Gamma \cdot \mathbb{E}[\widehat{\text{odds}}(X) | \widehat{\text{odds}}(X) \in I].$$

The expected odds is then estimated for each bin I by counting samples from the target and trial distributions. For all numerical experiments, we use 5 bins.

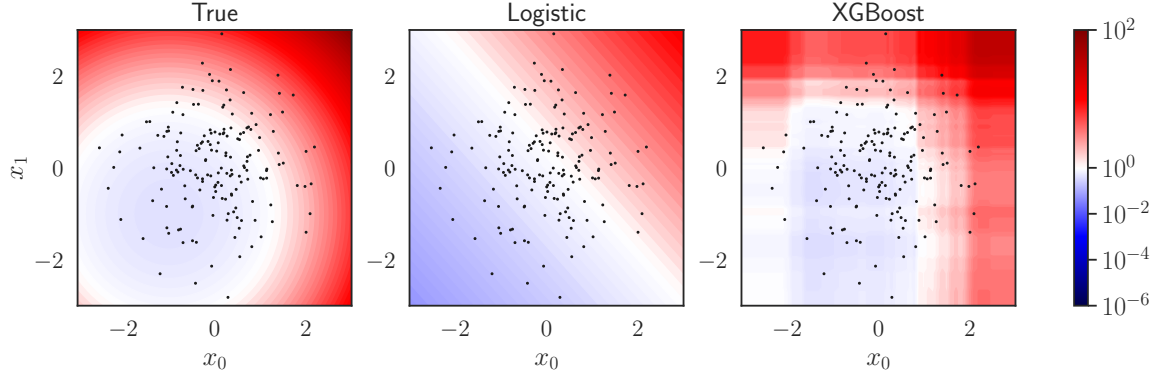
B.2 Synthetic data

We extend the experiments in Section 5.1 to include two extra target populations D, respective E. The full list of parameters used in (14) are given in Table 4.

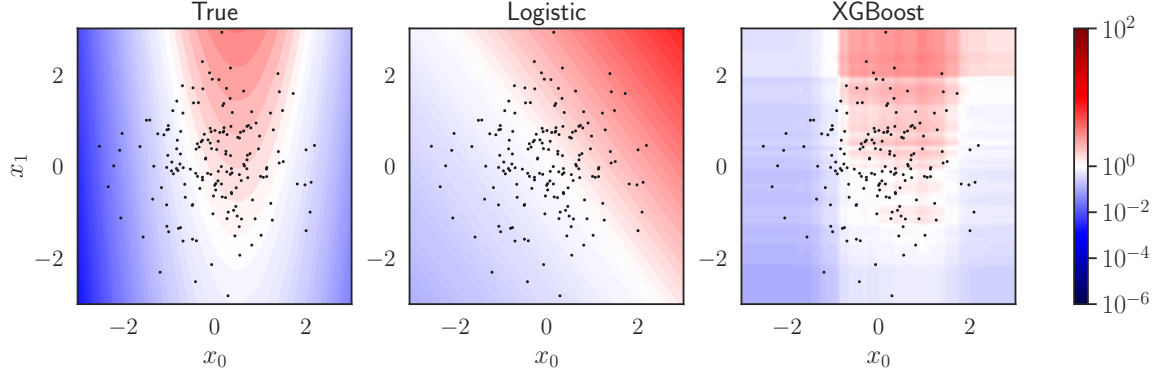
Figure 10 compares nominal sampling odds, $\text{odds}(X)$, obtained from the fitted models with the unknown odds, $\widehat{\text{odds}}(X)$, for the target populations C, D, respective E. In all these cases, the logistic model is misspecified and miscalibrated while the XGBoost model provides odds that resemble the true ones.

Table 4: Means and variances of covariate distribution $p(X|S)$ in (14).

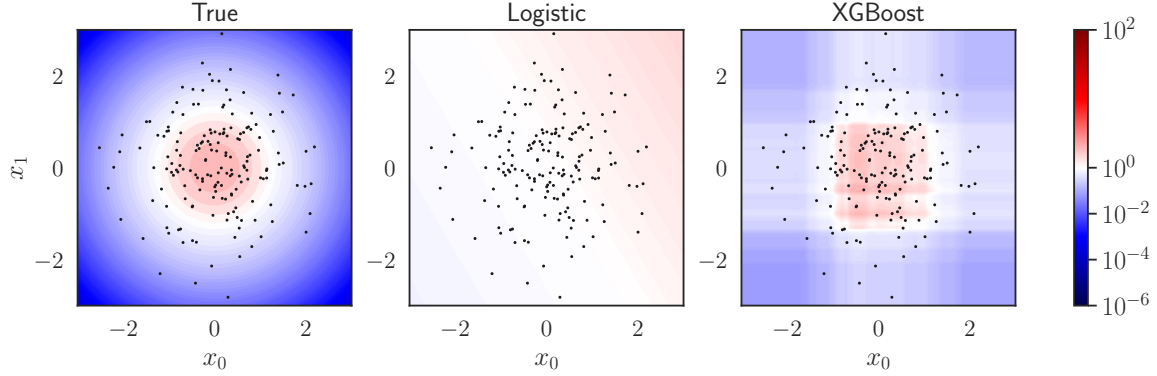
Population	$\mu_{0,S}$	$\mu_{1,S}$	$\sigma_{0,S}^2$	$\sigma_{1,S}^2$
A ($S = 0$)	0.5	0.5	1.0	1.0
B ($S = 0$)	0.0	0.0	1.5	1.5
C ($S = 0$)	0.5	0.5	1.5	1.5
D ($S = 0$)	0.25	0.25	0.5	1.0
E ($S = 0$)	0.0	0.0	0.5	0.5
Trial ($S = 1$)	0.0	0.0	1.0	1.0



(a) Sampling odds for target population C.



(b) Sampling odds for target population D.



(c) Sampling odds for target population E.

Figure 10: True sampling odds, $\text{odds}(X)$, compared with nominal odds, $\widehat{\text{odds}}(X)$, obtained from logistic and XGBoost models $\widehat{p}(S|X)$. The dots are a random subsample of the trial samples.

In Figure 11, we use the limit curves to evaluate the out-of-sample loss of a ‘treat all’ policy π_1 , i.e.

$$p_{\pi_1}(A = 0 \mid X) = 1,$$

for the target populations C, D, respective E. We start with population C in Figure 11a. The limit curve derived for the baseline closely align with the logistic model when $\Gamma = 1$, but is consistently slightly lower. For the certified curves the informativeness stays above 90% for odds miscalibration degrees $\Gamma \in [1, 1.5]$. For the miscoverage gap, the baseline and the misspecified logistic model for $\Gamma = 1$ are invalid, whereas the xgboost model has only a slight negative miscoverage gap. As the degree of miscalibration Γ increases to 1.5, all limit curves indicate positive miscoverage gaps. In Figure 11b, we evaluate the same policy π_1 , but for population D. Now, the limit curves modelled using the baseline and logistic regression infer consistently higher losses than the curves modelled using xgboost when $\Gamma = 1$. For the curve using the logistic model the informativeness stays above 90% for odds miscalibration degrees $\Gamma \in [1, 1.5]$. The same figure for the xgboost model is 95%. All the miscoverage gaps are positive, but the curves held with xgboost are tighter. Finally, in Figure 11c, we assess this for population E. The obtained limit curves are similar to the curves for population E but the informativeness stay above 95% for both models. Again, all the miscoverage gaps are positive, but the curves held with xgboost are tighter.

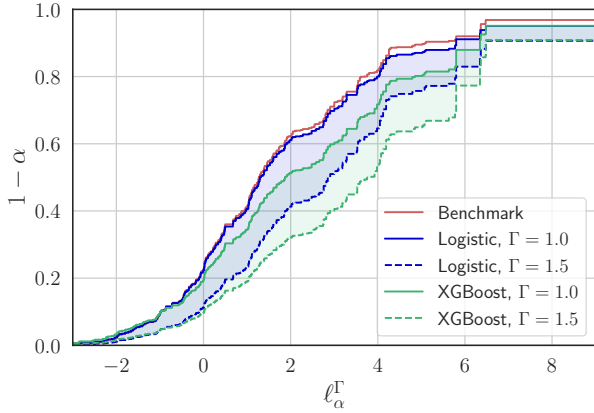
In Figure 12, we use reliability diagrams to assess and compare the performance of logistic and xgboost models of the nominal odds for the target populations C, D, and E, respectively. For target population C, it is evident that the xgboost model shows a closer alignment with the diagonal compared to the logistic model. This discrepancy motivates a higher value for the parameter Γ for the logistic model. This is in line with Figure 10a where the xgboost model is visually closer to the true model. For target populations D and E, both models deviate from the diagonal, although the xgboost model maintains a closer proximity to it when compared to the logistic model.

In Figure 13, we compare the ‘treat all’ policy with a ‘treat none’ policy, i.e.,

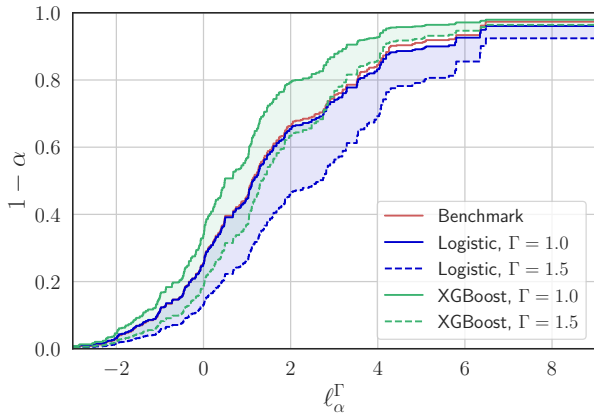
$$p_{\pi_0}(A = 0 \mid X) = 1,$$

for the target populations B, C, D and E. If their expected losses are estimated using (6), π_1 is the recommended choice over π_0 in all target populations. However, the tail losses certified for the ‘treat all’ policy π_0 are, specially for trial population B and C (Figure 13a and 13b), lower than the tail losses certified for π_1 .

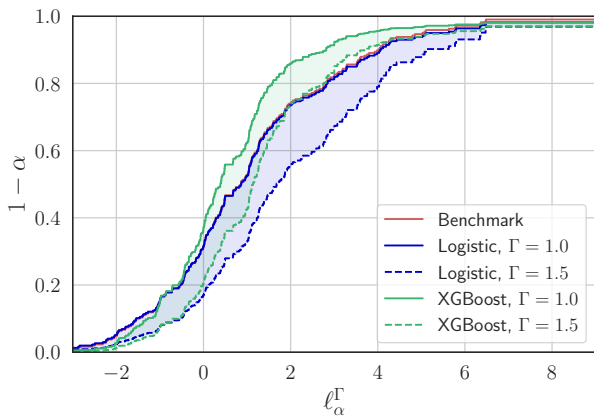
For completeness, the actual degree of miscalibration for all target populations are visualized in Figure 14.



(a) Limit curve and miscoverage gap for target population C.

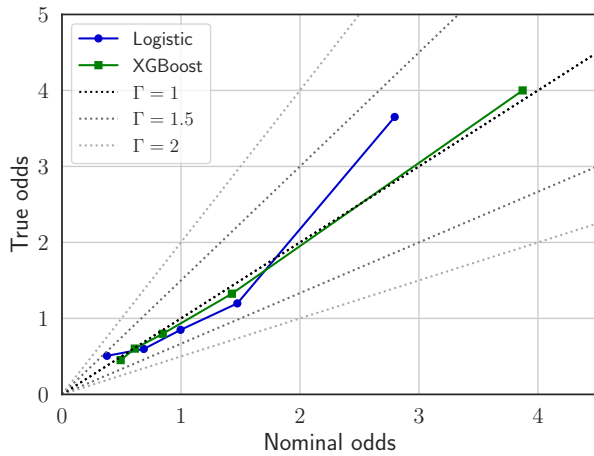


(b) Limit curve and miscoverage gap for target population D.

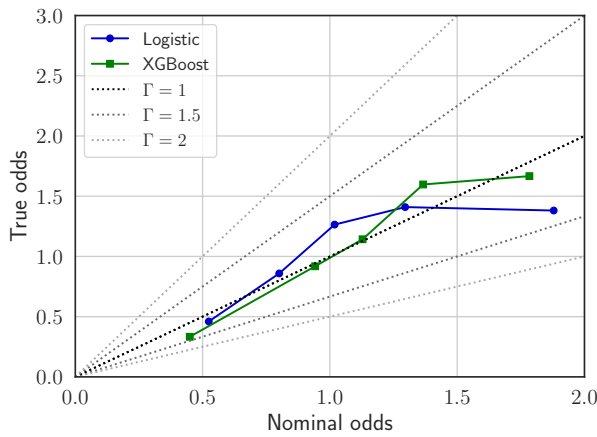


(c) Limit curve and miscoverage gap for target population E.

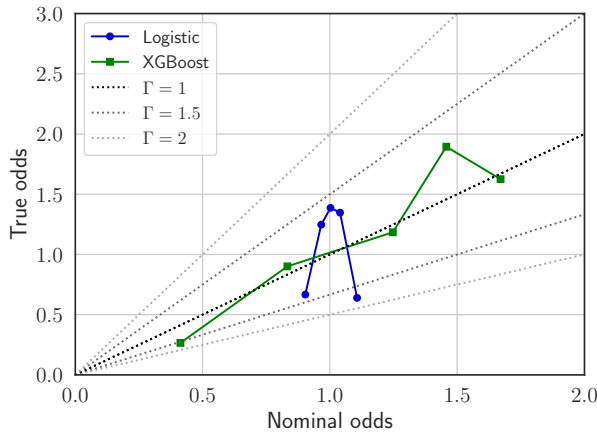
Figure 11: Evaluating ‘treat all’ policy π_1 for different target populations with degrees of miscalibration $\Gamma \in [1, 1.5]$.



(a) Reliability diagram for target population C.

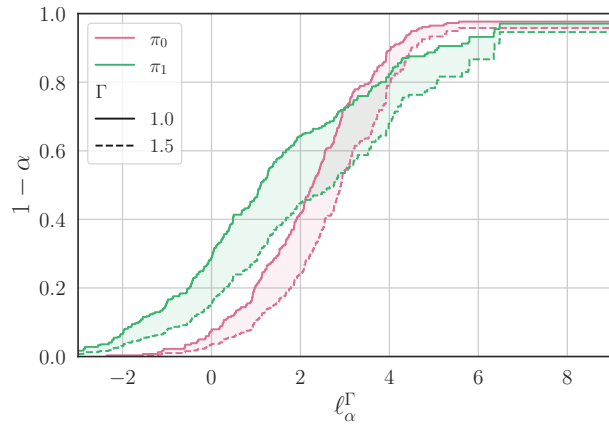


(b) Reliability diagram for target population D.

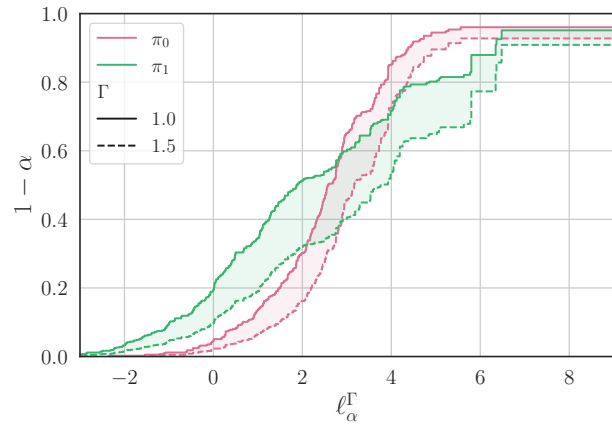


(c) Reliability diagram for target population E.

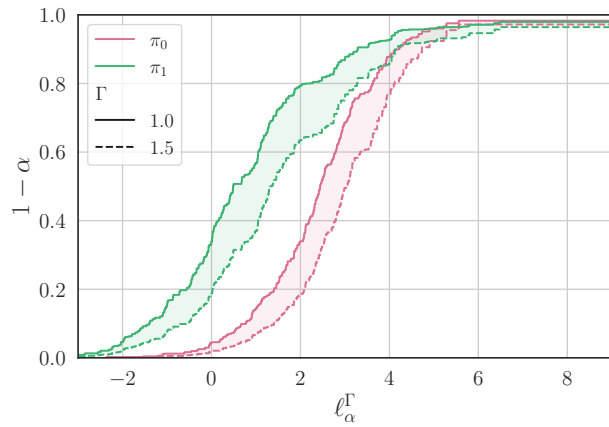
Figure 12: Reliability diagram of the observed odds against the average predicted nominal odds obtained from logistic and XGBoost-trained models.



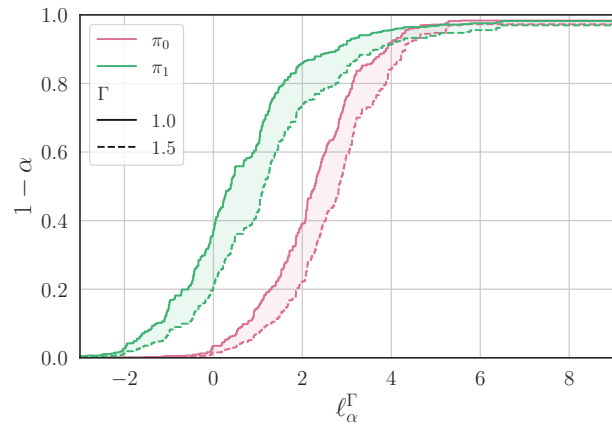
(a) Limit curves for target population B.



(b) Limit curves for target population C.



(c) Limit curves for target population D.



(d) Limit curves for target population E.

Figure 13: Limit curves for π_0 and π_1 for different target populations certified for $\Gamma \in [1, 1.5]$.

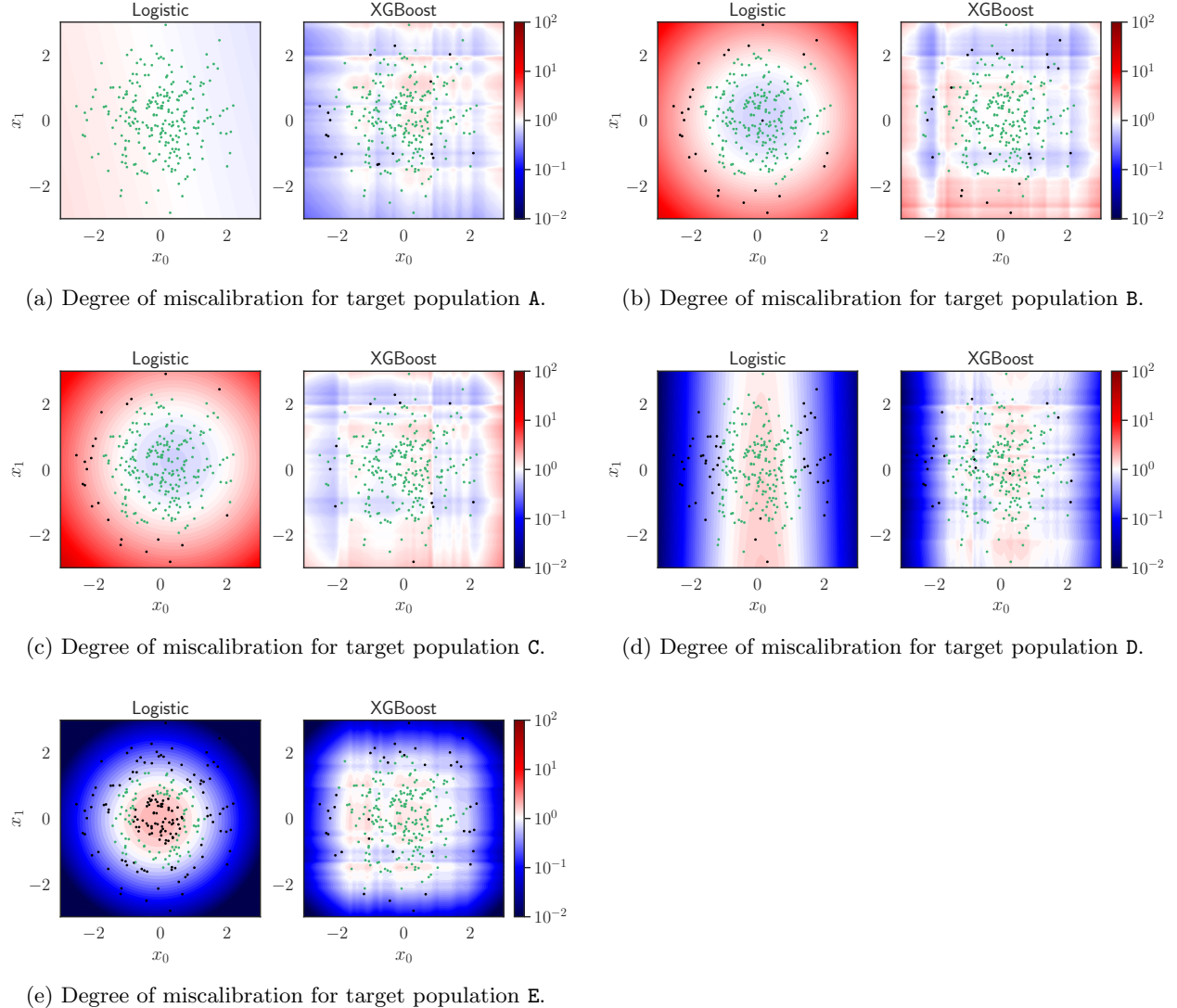


Figure 14: The actual degree of miscalibration for different target populations. The dots are a random subsample of the trial samples, where the green ones corresponds to a degree of miscalibration within $\Gamma = 1.5$ and the black ones to a degree of miscalibration not bounded by $\Gamma = 1.5$.